

Effect of Graphene on Growth of Neuroblastoma Cells

Park, Hye-Bin^{1†}, Hyo-Geun Nam^{2†}, Hong-Gi Oh², Jung-Hyun Kim¹, Chang-Man Kim³, Kwang-Soup Song^{2*}, and Kwang-Hwan Jhee^{1*}

¹Department of Applied Chemistry, Kumoh National Institute of Technology, Gumi 730-701, Korea

²Department of Medical IT Convergence Engineering, Kumoh National Institute of Technology, Gumi 730-701, Korea

³Gumi Electronics and Information Technology Research Institute, Biomedical IT Convergence Center, Gumi 730-701, Korea

Received: December 4, 2012 / Revised: December 12, 2012 / Accepted: December 14, 2012

The unique properties of graphene have earned much interest in the fields of materials science and condensed-matter physics in recent years. However, the biological applications of graphene remain largely unexplored. In this study, we investigated the conditions and viability of a cell culture exposed to graphene onto glass and SiO₂/Si, using a human nerve cell line, SH-SY5Y. Cell viability was 84% when cultured on glass and SiO₂/Si coated with graphene as compared with culturing on polystyrene surface. Fluorescence data showed that the presence of graphene did not influence cell morphology. These findings suggest that graphene may be used for biological applications.

Key words: Graphene, SH-SY5Y, AFM, Raman spectroscopy, cell viability

Carbon-based materials have been the focal point in recent years because of their unique properties, such as high thermal conductivity, low friction coefficient, wide band gap, excellent mechanical strength, chemical inertness, and high biocompatibility [4]. The bioindustry requires highly stable biomaterials to fabricate highly sensitive biosensors and artificial internal organs as orthopedic replacements [18, 20].

Graphene is a single-atom sheet of *sp*²-bonded carbon atoms in a closely packed honeycomb structure. It is one of the most attractive nanostructured materials with physical, chemical, and biological applications [3, 6, 12, 17]. Graphene combines surface stability with high corrosion resistance

and biotolerance, which are ideal features for medical applications, such as to construct biosensors, biomaterials, surgical tools, and medical implants [19]. In this work, we report the *in vitro* study of cell viability on a graphene sheet that was constructed using the chemical vapor deposition (CVD) method. Although previous studies provided preliminary quantitative and morphological evidence of cell interactions on graphene sheets, the biological responses of cells are still not clear and have not been sufficiently studied [8, 11, 14, 15]. The nervous system would be an ideal breakthrough model in terms of the biomedical applications of the graphene sheet, which has a non-doping surface conductivity [8, 18]. Human nerve SH-SY5Y cells are electroactive, and functions of the nervous system are based on electrical responses [11, 21]. Therefore, the determination of SH-SY5Y cell viability could be used as a method to characterize biocompatibility on a graphene sheet. The graphene sheets were prepared by the Samsung Co., Korea. In brief, the graphene sheet was deposited on a copper foil and then attached to a thin polymer film coated with an adhesive layer (thermal release tape) by passing between 2 rollers. The copper foil was removed by an electrochemical reaction with aqueous 0.1 M ammonium persulfate (APS) solution [(NH₄)₂S₂O₈]. Then the graphene sheet was detached from the thermal release tape and was released to the target substrate by thermal treatment. We used silicon (100, p-typed) and glass as the target substrates on which the monolayer graphene sheet was formed. All graphene sheets were used without any further surface functionalization for cell culture. The graphene films produced in our experiments exhibited an acceptable optical image of the graphene film transferred onto SiO₂/Si (Fig. 1A). The surface morphology and roughness of the graphene sheet were evaluated using an atomic force microscope (AFM, ParkSYSTEMS, XE-100). The root mean squared (R_q) roughness and peak roughness (R_{pv}) of the surface were evaluated using an AFM, which was

*Corresponding authors

K.-H. J.

Phone: +82-54-478-7837; Fax: +82-54-478-7710;
E-mail: khjhee@kumoh.ac.kr

K.-S. S.

Phone: +82-54-478-7435; Fax: +82-54-478-7445;
E-mail: kssong10@kumoh.ac.kr

†These authors contributed equally to this work.

operated in tapping mode in air at room temperature, and the scan size was $10\text{ }\mu\text{m} \times 10\text{ }\mu\text{m}$. When comparing the SiO_2/Si (001, p-typed) and graphene-coated SiO_2/Si (001, p-typed), there were some ripples and wrinkles in the AFM image on the graphene-coated SiO_2/Si , as shown in Fig. 1B. These ripples and wrinkles were intrinsic characteristics of the CVD-grown single-layer graphene [1, 5, 10]. The surface roughness [R_q] of the SiO_2/Si and graphene-coated SiO_2/Si was 0.287 nm and 0.491 nm , respectively. On the basis of the AFM data, the thickness of the deposited single-layer graphene film was determined to be approximately $0.6\text{--}0.9\text{ nm}$ through the y-axis [7]. Since the ripples and wrinkles were made by the largely transferred graphene sheet on the substrate, the thickness of the graphene sheet was higher than that of the single layer value of 0.4 nm . Raman spectroscopy is an efficient method for examining the crystal structure of carbon materials, such as graphene sheets. The single-, bi-, and multi-layer structures of graphene can also be evaluated using this technique [2]. Therefore, we characterized the carbon structure of the graphene sheet by Raman spectroscopy (Renishaw, System 1000) by using

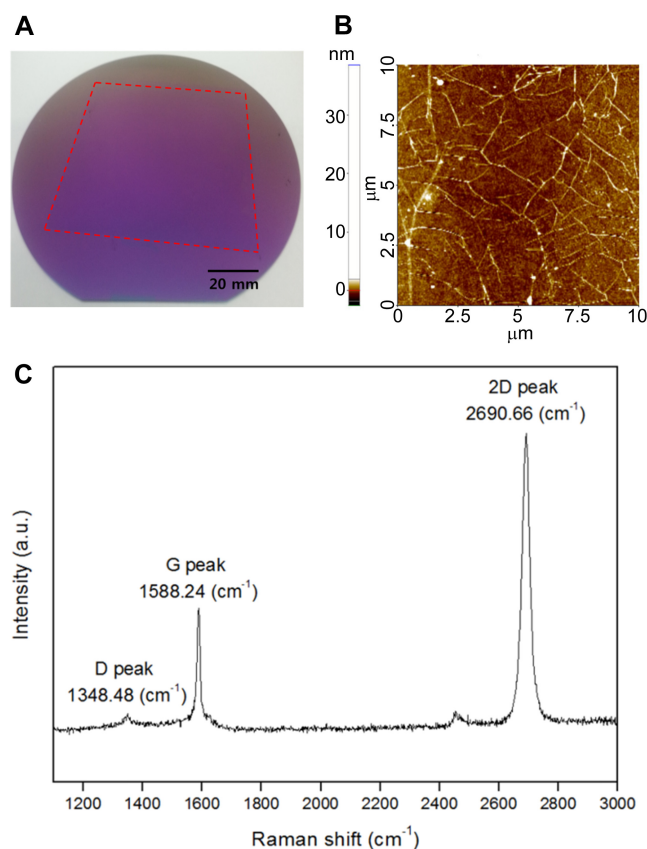


Fig. 1. Characterization of the chemical vapor deposition (CVD)-grown graphene film.

(A) Optical image of the graphene film after transfer to the SiO_2/Si . (B) AFM image of graphene upon SiO_2/Si transfer. (C) Raman spectrum of graphene (incident laser wavelength: 514 nm).

an Ar-ion laser at a wavelength of 514 nm . The Raman spectrum can be used to analyze graphene by determining the peak position and the G-to-2D intensity ratio (I_G/I_{2D}). The position of the G peak and the shape and position of the 2D peak are characteristic determinants of the graphene sheet layer [2, 7]. The G and 2D peaks of single-layer graphene are typically found at $1,585\text{ cm}^{-1}$ and $2,679\text{ cm}^{-1}$, respectively [2, 3, 22]. In this study, the G peak of graphene-coated SiO_2/Si was centered at 1588.24 cm^{-1} and the 2D peak at $2,690.66\text{ cm}^{-1}$, as shown in Fig. 1C. The intensity of the 2D peak (I_{2D} : 2903) was twice as large as the G peak intensity (I_G : 1152). The intensity ratio (I_G/I_{2D}) was $0.39 (<0.5)$, which indicates that the graphene exists as a large, single-layer sheet on the SiO_2/Si substrates [2]. However, AFM analysis also exhibited the slightly overlapping areas, bilayer islands, and multilayer islands (Fig. 1B). Our graphene sample also exhibited a very small D peak (Fig. 1C). The D peak indicates the defect of graphene on the Raman spectroscopy, and its intensity depends on the site of defect. On the basis of the 3 images in Fig. 1, we confirmed that the graphene was uniformly transferred to the substrates.

Cell viability was determined by a metabolic activity assay using 3-(4,5-dimethylthiazol-2-yl)-2,5-diphenyl-2H-tetrazolium bromide (MTT; Amresco, Canada) [11]. An MTT assay assesses the metabolic activity of cells on the basis of the ability of the mitochondrial succinate-tetrazolium reductase system in viable cells to convert the yellow dye to a purple-colored formazan compound. SH-SY5Y (50,000 cells/well, 48 wells) cells were seeded on each sample and cultured for 3 days. After incubation for 3 days, the graphene-coated glass and SiO_2/Si were transferred to wells of another plate and fresh medium was added ($180\text{ }\mu\text{l}$); then, $20\text{ }\mu\text{l}$ of MTT solution (5 mg/ml) was added to each well, followed by incubation. After incubation, the medium in each well was removed and $200\text{ }\mu\text{l}$ of DMSO was added to solubilize the insoluble formazan dye. The absorbance was measured at 540 nm by using an Agilent 8453 UV-visible spectrophotometer (Agilent Technology, USA). Cell culture polystyrene (CCPS) was used as a control. As shown in Fig. 2, SH-SY5Y cells exhibited approximately 84% viability on graphene-coated glass and SiO_2/Si compared with CCPS. Substrates bound to graphene did not greatly affect cell viability (Fig. 2). Mouse hippocampal cells and human mesenchymal stem cells also showed no significant differences in cell viability between cells cultured on graphene-coated and non-coated substrates [7]. However, a recent study has reported that pristine graphene triggers apoptosis in macrophage RAW264.7 cells through the MAPK and TGF- β signaling pathways [9].

We also investigated cell viability by using fluorescent dyes such as calcein AM and Hoechst 33342. Calcein AM emits green fluorescence by an active esterase reaction and

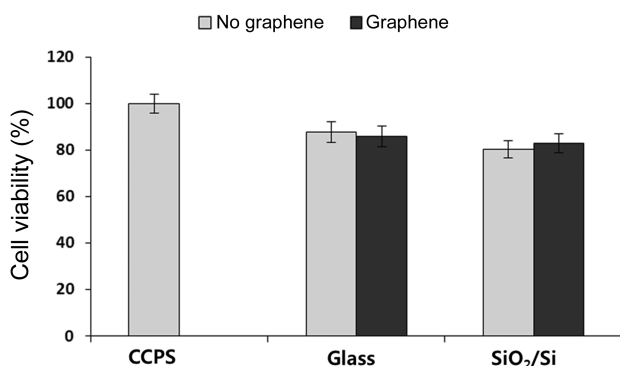


Fig. 2. SH-SY5Y cell viability after incubation for 3 days on different substrates.

The graph shows cell viability expressed as the percentage of cells grown on graphene-coated versus non-coated substrates normalized to cells grown on polystyrene (reference). CCPS represents cell culture polystyrene. Data are expressed as the mean \pm SD of 3 independent experiments performed in duplicate.

Hoechst 33342 emits blue fluorescence by binding to nuclear DNA [13, 16]. As shown in Fig. 3, SH-SY5Y cells showed mostly green staining in the 4 samples (glass, SiO_2/Si ,

glass coated with graphene, and SiO_2/Si coated with graphene). These data indicate that cells can survive on both substrates and graphene. There was no noticeable morphological difference in the cells cultured on non-coated and coated graphene surfaces. Our data suggest that graphene coating on different substrates can be used to develop biocompatible materials that can be used *in vitro*.

Taken together, our data reveal that graphene exhibited excellent biocompatible properties in terms of cell viability and morphology. Therefore, graphene can be useful in applications such as fabrication of biological sensors, biomolecular patterning, and for studying cell-surface interactions. Our data support the potential of graphene as a material for neural interfacing and provides insight into the future biomedical applications of carbon-based materials.

Acknowledgments

This research was supported by the Basic Science Research Program through the National Research Foundation of Korea (NRF) funded by the Ministry of Education, Science and Technology (2011-0011909).

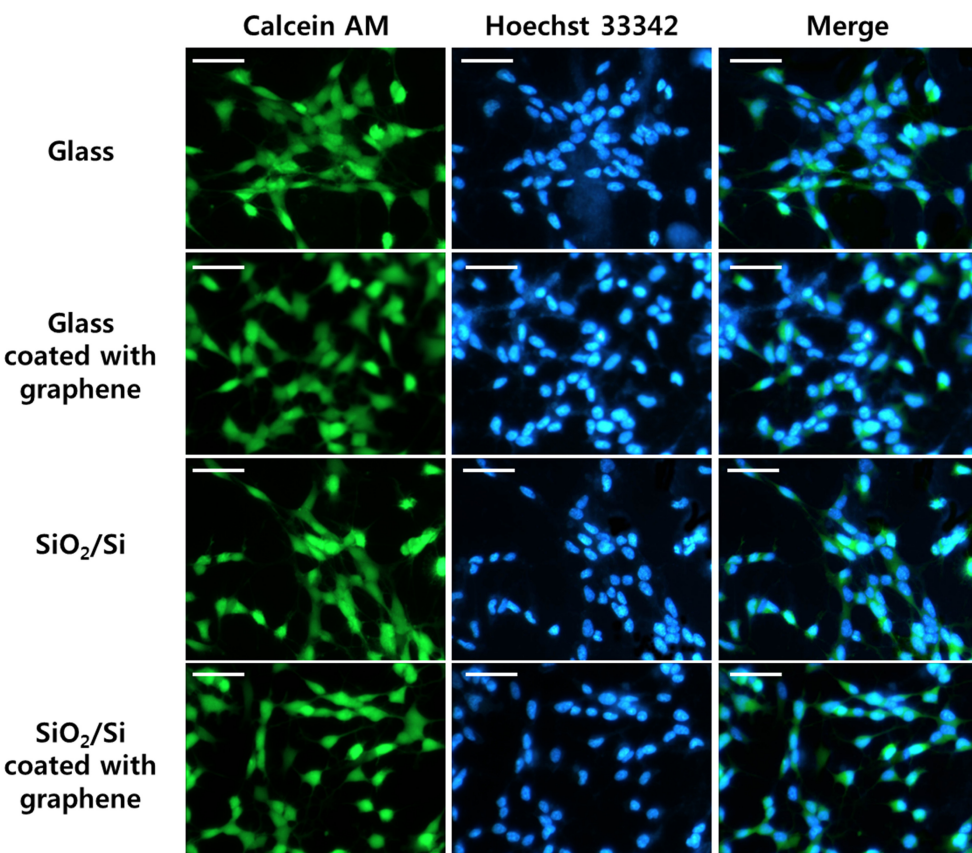


Fig. 3. Morphology of SH-SY5Y cells grown on different substrates. Cells were stained with Hoechst 33342 and calcein AM. Scale bars are 50 μm .

REFERENCES

- Bae, S., H. Kim, Y. Lee, X. Xu, J. S. Park, Y. Zheng, et al. 2010. Roll-to-roll production of 30-inch graphene films for transparent electrodes. *Nat. Nanotechnol.* **5**: 574–578.
- Ferrari, A. C., J. C. Meyer, V. Scardaci, C. Casiraghi, M. Lazzari, F. Mauri, et al. 2006. Raman spectrum of graphene and graphene layers. *Physic. Rev. Lett.* **97**.
- Gomez-Navarro, C., R. T. Weitz, A. M. Bittner, M. Scolari, A. Mews, M. Burghard, and K. Kern. 2007. Electronic transport properties of individual chemically reduced graphene oxide sheets. *Nano. Lett.* **7**: 3499–3503.
- Jia, G., H. Wang, L. Yan, X. Wang, R. Pei, T. Yan, et al. 2005. Cytotoxicity of carbon nanomaterials: Single-wall nanotube, multi-wall nanotube, and fullerene. *Environ. Sci. Technol.* **39**: 1378–1383.
- Jo, S. B., J. Park, W. H. Lee, K. Cho, and B. H. Hong. 2012. Large-area graphene synthesis and its application to interface-engineered field effect transistors. *Solid State Commun.* **152**: 1350–1358.
- Katsnelson, M. I. and K. S. Novoselov. 2007. Graphene: New bridge between condensed matter physics and quantum electrodynamics. *Solid State Commun.* **143**: 3–13.
- Kudin, K. N., B. Ozbas, H. C. Schniepp, R. K. Prud'homme, I. A. Aksay, and R. Car. 2008. Raman spectra of graphite oxide and functionalized graphene sheets. *Nano. Lett.* **8**: 36–41.
- Li, N., X. Zhang, Q. Song, R. Su, Q. Zhang, T. Kong, et al. 2011. The promotion of neurite sprouting and outgrowth of mouse hippocampal cells in culture by graphene substrates. *Biomaterials* **32**: 9374–9382.
- Li, Y., Y. Liu, Y. Fu, T. Wei, L. Le Guyader, G. Gao, et al. 2012. The triggering of apoptosis in macrophages by pristine graphene through the MAPK and TGF-beta signaling pathways. *Biomaterials* **33**: 402–411.
- Lim, W. S., Y. Y. Kim, H. Kim, S. Jang, N. Kwon, B. J. Park, et al. 2012. Atomic layer etching of graphene for full graphene device fabrication. *Carbon* **50**: 429–435.
- Lv, M., Y. Zhang, L. Liang, M. Wei, W. Hu, X. Li, and Q. Huang. 2012. Effect of graphene oxide on undifferentiated and retinoic acid-differentiated SH-SY5Y cells line. *Nanoscale* **4**: 3861–3866.
- Meyer, J. C., A. K. Geim, M. I. Katsnelson, K. S. Novoselov, T. J. Booth, and S. Roth. 2007. The structure of suspended graphene sheets. *Nature* **446**: 60–63.
- Mocharla, R., H. Mocharla, and M. E. Hodes. 1987. A novel, sensitive fluorometric staining technique for the detection of DNA in RNA preparations. *Nucleic Acids Res.* **15**: 10589.
- Nayak, T. R., H. Andersen, V. S. Makam, C. Khaw, S. Bae, X. Xu, et al. 2011. Graphene for controlled and accelerated osteogenic differentiation of human mesenchymal stem cells. *ACS Nano.* **5**: 4670–4678.
- Park, S. Y., J. Park, S. H. Sim, M. G. Sung, K. S. Kim, B. H. Hong, and S. Hong. 2011. Enhanced differentiation of human neural stem cells into neurons on graphene. *Adv. Mater.* **23**: H263–H267.
- Patel, H., C. Tscheika, and H. Heerklotz. 2009. Characterizing vesicle leakage by fluorescence lifetime measurements. *Soft Matter* **5**: 2849–2851.
- Shang, N. G., P. Papakonstantinou, M. McMullan, M. Chu, A. Stamboulis, A. Potenza, et al. 2008. Catalyst-free efficient growth, orientation and biosensing properties of multilayer graphene nanoflake films with sharp edge planes. *Adv. Funct. Mater.* **18**: 3506–3514.
- Vittorio, O., V. Raffa, and A. Cuschieri. 2009. Influence of purity and surface oxidation on cytotoxicity of multiwalled carbon nanotubes with human neuroblastoma cells. *Nanomedicine* **5**: 424–431.
- Weng, H. A., C. C. Wu, C. C. Chen, C. C. Ho, and S. J. Ding. 2010. Preparation and properties of gold nanoparticle-electrodeposited titanium substrates with Arg-Gly-Asp-Cys peptides. *J. Mater. Sci. Mater. Med.* **21**: 1511–1519.
- Wu, L., H. S. Chu, W. S. Koh, and E. P. Li. 2010. Highly sensitive graphene biosensors based on surface plasmon resonance. *Opt. Express* **18**: 14395–14400.
- Xun, Z., D. Y. Lee, J. Lim, C. A. Canaria, A. Barnebey, S. M. Yanonne, and C. T. McMurray. 2012. Retinoic acid-induced differentiation increases the rate of oxygen consumption and enhances the spare respiratory capacity of mitochondria in SH-SY5Y cells. *Mech. Ageing Dev.* **133**: 176–185.
- Yang, D., A. Velamakanni, G. Bozoklu, S. Park, M. Stoller, R. D. Piner, et al. 2009. Chemical analysis of graphene oxide films after heat and chemical treatments by X-ray photoelectron and Micro-Raman spectroscopy. *Carbon* **47**: 145–152.